

# Aspects for efficient wide spectral band THz generation via CO<sub>2</sub> laser down conversion

Yu.N. Panchenko<sup>1</sup>, Yu.M. Andreev<sup>2,3</sup>, G.V. Lanski<sup>2,3</sup>, V.F. Losev<sup>1,4</sup>, D.M. Lubenko<sup>1</sup>

<sup>1</sup>Gas Lasers Laboratory, High Current Electronic Institute of SB RAS, 2/3 Akademicheskii Ave., Tomsk 634055, Russia

*e-mail: lideru@gmail.com*

<sup>2</sup>Laboratory of Geosphere-Biosphere Interactions, Institute of Monitoring of Climatic and Ecological Systems SB RAS, 10/3, Akademicheskii Ave., Tomsk, 634055, Russia

<sup>3</sup>Laboratory of Advanced Materials and Technologies, Siberian Physical-Technical Institute of Tomsk State University, 1, Novosobornaya Sq., Tomsk, 634050, Russia

<sup>4</sup>Tomsk Polytechnic University, 30 Lenin Ave., Tomsk, 634034, Russia

## ABSTRACT

Detailed model study of THz generation by CO<sub>2</sub> laser down-conversion in pure and solid solution crystals GaSe<sub>1-x</sub>S<sub>x</sub> is carried out for the first time. Both forward and backward collinear interactions of common (eo-e, oe-e, oe-o, oo-e, ee-o) and original (ee-e, oo-o) types are considered. Possibility of realization, phase matching angles and figure of merits are estimated for line mixing within 9 μm and 10 μm emission bands, as well between them. Dispersion properties of o- and e-wave refractive indices and absorption coefficients for GaSe, GaS and GaSe<sub>1-x</sub>S<sub>x</sub> crystals were preliminary measured by THz-TDS, approximated in the equation form and then used in the study. Estimated results are presented in the form of 3-D figures that are suitable for rapid analyses of DFG parameters. The most efficient type of interaction is eo-o type. Optimally doped (x = 0.09-0.13) GaSe<sub>1-x</sub>S<sub>x</sub> crystals are from 4 to 5 times more efficient at limit pump intensity than not doped GaSe crystals.

**Keywords:** GaSe, GaSe<sub>1-x</sub>S<sub>x</sub>, parametric frequency conversion, phase matching, figure of merit, THz

## 1. INTRODUCTION

Frequency conversion can significantly extend application of wide-distributed high power CO<sub>2</sub> lasers. Efficient frequency conversion of TEA CO<sub>2</sub> lasers into THz range is of special interest due to possible numerous applications. Transparency windows of the atmosphere allow operation of remote differential absorption detection & composition identification systems. THz transparency windows of the atmosphere are located, for example, at central frequencies of 0.85 and 1.5 THz<sup>1</sup>. Existing of well resolved absorption spectra of non-conductive solid matters and non-polar liquids within THz atmospheric transparency windows in line with well resolved absorption spectra of gases additionally stimulates design of THz remote sensing systems. Low energy THz quanta allow carrying out dangerousness remote control of matters on the human body (explosives, drugs, toxic gases in containers) candid in clothes, synthetic matters and goods made of variety of natural materials due to their transparency. THz range is also attractive for condition analyzes of biological objects *in vivo*. These circumstances further support design of efficient CO<sub>2</sub> laser frequency converters into THz range as well as THz remote sensing systems.

Application of asymmetric nonlinear crystals as parametric frequency converters of CO<sub>2</sub> lasers is preferable because phase matching (PM) of interactive waves can be achieved and frequency conversion efficiency maximized consequently. However, there is limited number of asymmetric inorganic nonlinear crystals suitable for THz applications that always possess much higher damage threshold to that for organic crystals. Higher pump intensity is resulting in higher conversion efficiency. Mostly suitable inorganic acentrosymmetric crystals for THz frequency converters are ZnGeP<sub>2</sub><sup>2,3,4</sup>, ε-GaSe<sup>3,5</sup>, AgGaSe<sub>2</sub><sup>3,6</sup>, AgGa<sub>1-x</sub>In<sub>x</sub>Se<sub>2</sub><sup>3,6</sup> and Tl<sub>3</sub>AsSe<sub>3</sub><sup>7</sup> crystals. Among them, GaSe crystal is of extra interest due to extreme physical properties.

The extreme physical properties of GaSe: wide transparency range, large birefringence, damage threshold and thermal conductivity have been successfully employed to generate coherent radiation from the near IR (0.7895 μm) through the mid-IR and further through the entire terahertz (THz) range up to the sub-centimeter wavelength 5640 μm<sup>8,9,4</sup>. Many of

the unique properties of GaSe are associated with its layered structure. The basic four-fold layer consists of two monoatomic sheets of Ga sandwiched between two monoatomic sheets of Se. The strong covalent interaction within the atomic layers and weak, Van-der-Waals type bonding between basic layers, renders GaSe as a highly anisotropic material. On the other hand, the layer structure results in extreme low hardness (almost zero by Mohs scale) and easy cleaving along planes parallel to the atomic layers, and finally in hampering out-of-door large-area crystals applications.

Fortunately, an original  $\epsilon$ -polytype structure of GaSe is strengthening by isovalent element doping as well other physical properties responsible for frequency conversion efficiency are modifying that, respectively, allowed easier cut & polishing at arbitrary directions and improves in the frequency conversion efficiency. Strengthened structure gives opportunity of the application in out-of-door applied systems<sup>10</sup>. Modified properties and improved efficiencies are reported for a number of doped crystals: light (GaSe:S) and heavily S-doped GaSe crystals or so called solid solution crystals GaSe<sub>1-x</sub>S<sub>x</sub> (GaSe:GaS)<sup>11,12,13,14,15</sup>, GaSe:In and Ga<sub>1-x</sub>In<sub>x</sub>Se<sup>16,17,18,19,20</sup>, GaSe:Te and GaSe<sub>1-x</sub>Te<sub>x</sub><sup>18,21,22</sup>, doped GaSe:Er<sup>23,24</sup> and GaSe:Al<sup>25</sup> crystals. Increased frequency conversion efficiency is recorded for frequency conversion into both mid-IR<sup>12,16,17,19</sup> and THz<sup>26,27,28</sup> range.

Due to a set of modified parameters: increased damage threshold, decreased phase matching angle, lower absorption and refraction, short-wavelength shifted transparency and phase matching ranges etc. the highest frequency conversion efficiency was recorded for solid solution GaSe<sub>1-x</sub>S<sub>x</sub> crystals<sup>12,27,28</sup>. In particular, for Er<sup>3+</sup>:YAG laser SHG conversion efficiency in optimally composition GaSe<sub>1-x</sub>S<sub>x</sub> crystal was of 2.4 times higher to that for pure GaSe crystal, as well as for THz generation by Ti:Sapphire laser frequency down-conversion. In contradiction, negative effects of S-doping on the optical damage threshold and on frequency conversion efficiency were also reported<sup>15,29</sup>, that reflect doping-induced degradation in optical quality.

In fact, differences in the state-of-the-art of growth technology, limited distribution of doped GaSe crystals and still problematic cut & high optical quality polishing of pure and doped GaSe crystals are reasons of paucity and highly scattered data on optical properties of pure and doped GaSe crystals in THz range. Due to limited distribution and processing absorption spectra for e-wave in GaSe<sub>1-x</sub>S<sub>x</sub> crystals (i.e. absorption anisotropy properties) in the THz range have only been studied for two solid solution compositions: GaSe<sub>0.71</sub>S<sub>0.29</sub><sup>15</sup> and GaSe<sub>0.74</sub>S<sub>0.26</sub><sup>14</sup>. From data in these studies and from measurements at fixed frequencies<sup>4,28</sup> it was established that the absorption coefficient  $\alpha_o$  exceeds  $\alpha_c$  at THz frequencies as it does in the pure GaSe crystal. This difference in absorption loss leads to a higher efficiency of THz e-wave generation<sup>9,28</sup>. It was also predicted and confirmed experimentally that the uncommon ee-e type of interaction can be realized in pure and S-doped GaSe crystals<sup>14,15</sup>.

Successful design of THz sources calls for adequate data on PM possibilities and potential efficiencies for all possible three frequency interactions. In turn, it needs in correct data on dispersion properties and absorption spectra over the entire transparency range for pure and S-doped GaSe and solid solution GaSe<sub>1-x</sub>S<sub>x</sub> crystals as a function of the mixing ratio. Correct data are a crucial factor in the selection of the most efficient type of three frequency interactions and in maximizing the frequency conversion efficiency. In the present work, we report for the first time to our knowledge detailed model study of all types of three frequency interactions in high optical quality GaSe<sub>1-x</sub>S<sub>x</sub>, x=0, 0.05, 0.11, 0.22, 0.29, 0.44 crystals: common (eo-e, oe-e, oe-o, oo-e, ee-o) and as well original (ee-e, oo-o) types. High quality crystals were grown by modified syntheses and single crystal growth technologies.

## 2. CRYSTAL GROWTH AND CHARACTERIZATION

A modified synthesis of polycrystalline material and the vertical Bridgman single crystal growth method were employed to grow single crystals of solid solution GaSe<sub>1-x</sub>S<sub>x</sub>. The starting materials for the synthesis were Ga 99.9997, Se 99.99 and S 99.95. The stoichiometric charge of Ga and Se, and the nominal 0, 1.1, 2.5, 5, 7, 11 mass.% S (x=0, 0.05, 0.11, 0.22, 0.29, 0.44, 1) was weighed out with an accuracy of  $\pm 0.1$  mg. Synthesis ampoules were loaded up to 65% in volume to minimize the quantity of residual gases and cosequent interaction so as to improve optical quality. Other details on the synthesis process are reported elsewhere<sup>30</sup>. After several hours of melt homogenization during the synthesis process, the temperature was slowly decreased to 40 K below the melting point of 1238 K of the compound at the rate of  $\sim 10$  K/h. Synthesised polycrystalline material GaSe is shown in Fig. 1a.

For the growth process, the polycrystalline material was loaded into a single wall cylindrical ampoule. The internal surface had a layer of pyrolytic carbon which protected the melt from reaction with the ampoule wall material and impurities. The unseeded crystal growth was performed by the vertical Bridgman method with heat field symmetry change and the symmetry center moving all over the oven space that is described elsewhere<sup>31,32</sup>. The sealed growth ampoule was loaded into a furnace having a temperature gradient of  $\sim 15$  K/cm at the estimated level of crystallization front. After homogenization of the melt at the temperature 30 K above the melting point, the ampoule was mechanically

lowered at the speed of 10 mm/day. No eutectic was found by visual examination. The boule allows easy sample cleaving with high quality surfaces up until the end section.

Two types of  $\text{GaSe}_{1-x}\text{S}_x$  samples were fabricated for the present study. The first type was cleaved from as-grown boules, i.e. it had faces orthogonal to the c-axis, so that a beam traversing the sample travelled parallel to the c-axis. The high optical quality of these samples can be estimated by the naked eye, evident in their transparency and homogeneity. The second type was mechanically cut and polished. These samples were made by first immersing a section of the  $\text{GaSe}_{1-x}\text{S}_x$  boule in monomer (polymetil crylate) mixed with a thermoinitiator and placed in an oven for polymerization for 2 hours. Once set, the boule section was cut perpendicular to the growth layers ( $\perp \bar{c}$ ) and then polished with fine 0.8-1.2  $\mu\text{m}$  POLIRIT™ abrasive (a versatile powder for polishing, based on a mixture of oxides of rare earth elements Ce, La, Nd), so that a traversing beam would travel orthogonally to the c-axis. The produced samples of both types were free from precipitates, voids or micro bubbles, or other visual defects.

Optical properties in mid-IR range were studied by using commerce spectrophotometers but THz-TDS (time-domain spectroscopy) measurements of o- ( $\alpha_o$ ) and e-wave ( $\alpha_e$ ) absorption coefficient spectra and absorption anisotropy in the 0.3-4.0 THz range for solid solution crystals  $\text{GaSe}_{1-x}\text{S}_x$  as it is described in details elsewhere<sup>33</sup>. It was found that grown crystals possesses from 2 to 3 times lower absorption coefficient that crystals grown by common syntheses and single crystal growth technology.

### 3. Model study

In this study both forward and backward three wave interactions were considered in accordance with Fig. 1.

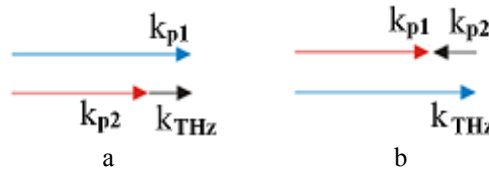


Fig. 1. Optical set-up for (a) forward and (b) backward three frequency interactions, where  $k_{p1}$ ,  $k_{p2}$ ,  $k_{\text{THz}}$  are wavenumbers of the pump line 1, pump line 2 and difference frequency (THz) emission, respectively.

For calculations, dispersion properties for GaS and GaSe were measured in THz range and approximated in the form of dispersion equations all through transparency range. Available data for from visible to through mid-IR were also used in approximation as it was presented<sup>33</sup>. Dispersion equations designed for GaS are as follows:

$$n_o^2 = -\frac{0.01129}{\lambda^6} + \frac{0.03648}{\lambda^4} + \frac{0.51402}{\lambda^2} + 6.59624 + \frac{2.71047\lambda^2}{\lambda^2 - 1025.42116} \quad (1)$$

$$n_e^2 = \frac{0.0113}{\lambda^6} + \frac{0.10569}{\lambda^4} - \frac{0.44573}{\lambda^2} + 4.92144 + \frac{0.315\lambda^2}{\lambda^2 - 720.12225}$$

Dispersion equations designed for GaSe are close to that<sup>34</sup>:

$$n_e^2 = 5.76 + \frac{0.3879}{\lambda^2} - \frac{0.2288}{\lambda^4} + \frac{0.1223}{\lambda^6} + \frac{0.4206\lambda^2}{\lambda^2 - 1780.3} \quad (2)$$

$$n_e^2 = 5.76 + \frac{0.3879}{\lambda^2} - \frac{0.2288}{\lambda^4} + \frac{0.1223}{\lambda^6} + \frac{0.4206\lambda^2}{\lambda^2 - 1780.3}$$

Dispersion for solid solution crystals grown from identical structure parent crystals were estimated by using the well-known relation<sup>35</sup>, adapted to the case of  $\varepsilon\text{-GaSe}_{1-x}\text{S}_x$ , as:

$$n_{o,e}^2(\varepsilon\text{-GaSe}_{1-x}\text{S}_x) = (1-x) \cdot n_{o,e}^2(\varepsilon\text{-GaSe}) + x \cdot n_{o,e}^2(\varepsilon\text{-GaS}) \quad (3)$$

Phase matching angles for difference frequency generation (DFG) were calculated by using common relations. For example, for oo-e interaction the relation is:

$$\frac{n_o(\lambda_{p1})}{\lambda_{p1}} - \frac{n_o(\lambda_{p2})}{\lambda_{p2}} = \pm \frac{n_o(\lambda_{THz}, \theta)}{\lambda_{THz}}, \quad (4)$$

where

$$\frac{1}{\lambda_{p1}} = \frac{1}{\lambda_{p2}} + \frac{1}{\lambda_{THz}}, \quad (5)$$

sign “+” and “-“ are related, respectively, to forward and backward waves, wavelengths are in  $\mu\text{m}$ . DFG efficiency is calculated by using relation<sup>36</sup>:

$$\frac{P_{THz}}{P_{p1}} = 2 \left( \frac{\mu_0}{\varepsilon_0} \right)^{1/2} \frac{\omega_3^2 d_{eff}^2 L^2}{n_1 n_2 n_3 c^2} \left( \frac{P_{p2}}{A} \right) T_1 T_2 T_3 e^{-\alpha_3 L} \frac{1 + e^{-\Delta\alpha L} - 2e^{-\Delta\alpha L/2} \cos(\Delta k L)}{(\Delta k L)^2 + \left( \frac{\Delta\alpha L}{2} \right)^2} \quad (6)$$

where  $\mu_0 = 4\pi \cdot 10^{-7}$  H/m is the magnetic permeability,  $\varepsilon_0 = 8.854 \cdot 10^{-12}$  F/m is the dielectric susceptibility,  $P_2/A = 50$  MW/cm<sup>2</sup> =  $5 \cdot 10^{11}$  MW/m<sup>2</sup> is pump intensity,  $\Delta k$  is phase mismatch that is equal to 0 at full phase matching), L is a crystal length in mm. Measured mid-IR absorption coefficient spectra  $\alpha$  for GaSe are approximated as

$$\alpha_{1,2} = \begin{cases} 0.00848\lambda + 0.20264 & (o) \\ 0.1839\lambda - 0.90666 & (e) \end{cases}, \quad [9.09-1.28 \mu\text{m}] \quad (7)$$

and THz absorption spectra as

$$\alpha_3 = \begin{cases} \frac{548.673}{\lambda} + 1.77357 & (o) \\ \frac{97.914}{\lambda} + 0.21373 & (e) \end{cases}, \quad [0.25-3.5 \text{ THz}]. \quad (8)$$

Here  $\alpha \text{ cm}^{-1} = \alpha \cdot 10^2 \text{ m}^{-1}$ ;  $\Delta\alpha = |\alpha_1 + \alpha_2 - \alpha_3|$ ;  $c = 3 \cdot 10^8$  m/s is light speed in vacuum,  $T_i = 4n_i / (n_i + 1)^2$ ,  $n_i$  are refractive indices at interacting wavelengths,  $\omega_3 = 2\pi\nu = 2\pi \cdot 300/\lambda$  THz =  $2\pi \cdot 300/\lambda \cdot 10^{12}$  Hz is THz frequency,  $d_{eff} \text{ pm/V} = d_{eff} \cdot 10^{-12} \text{ m/V}$  is second order nonlinear susceptibility coefficient. For o+o  $\rightarrow$  e, o+e  $\rightarrow$  e, e+e  $\rightarrow$  e and o+o  $\rightarrow$  o type of interactions relations for  $d_{eff}$  are, respectively:

$$d_{eff} = -d_{22} \cos\theta \sin 3\varphi \quad (9)$$

$$d_{eff} = d_{22} \cos^2\theta \cos 3\varphi \quad (10)$$

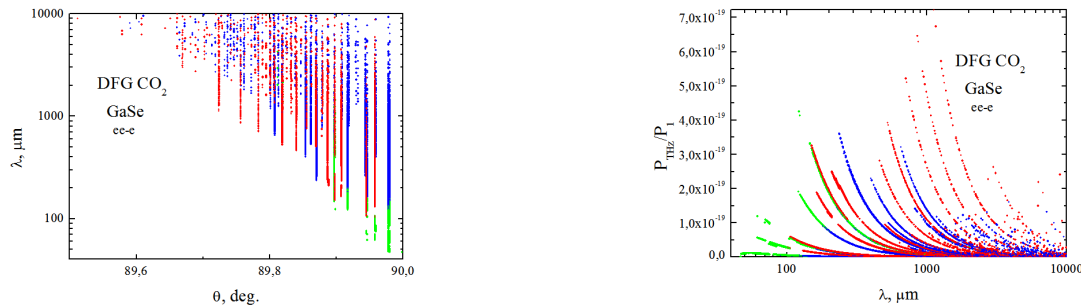
$$d_{eff} = d_{22} \cos^3\theta \sin 3\varphi \quad (11)$$

$$d_{eff} = -d_{22} \cos 3\varphi \quad (12)$$

Calculations are carried out for DFG in 5 mm GaSe and GaSe<sub>1-x</sub>S<sub>x</sub> under 50 MW/cm<sup>2</sup> and limit<sup>32,37</sup> pump intensities. CO<sub>2</sub> laser emission lines within from 9.09349 to 9.99177  $\mu\text{m}$  and from 10.01538 to 11.28093  $\mu\text{m}$  and their spectral dependences have been considered in the calculations carried out.

#### 4. Results and discussion

Calculated data are presented in the figures below. DFG PM and related frequency conversion efficiencies are plotted in Fig. 2, 4.



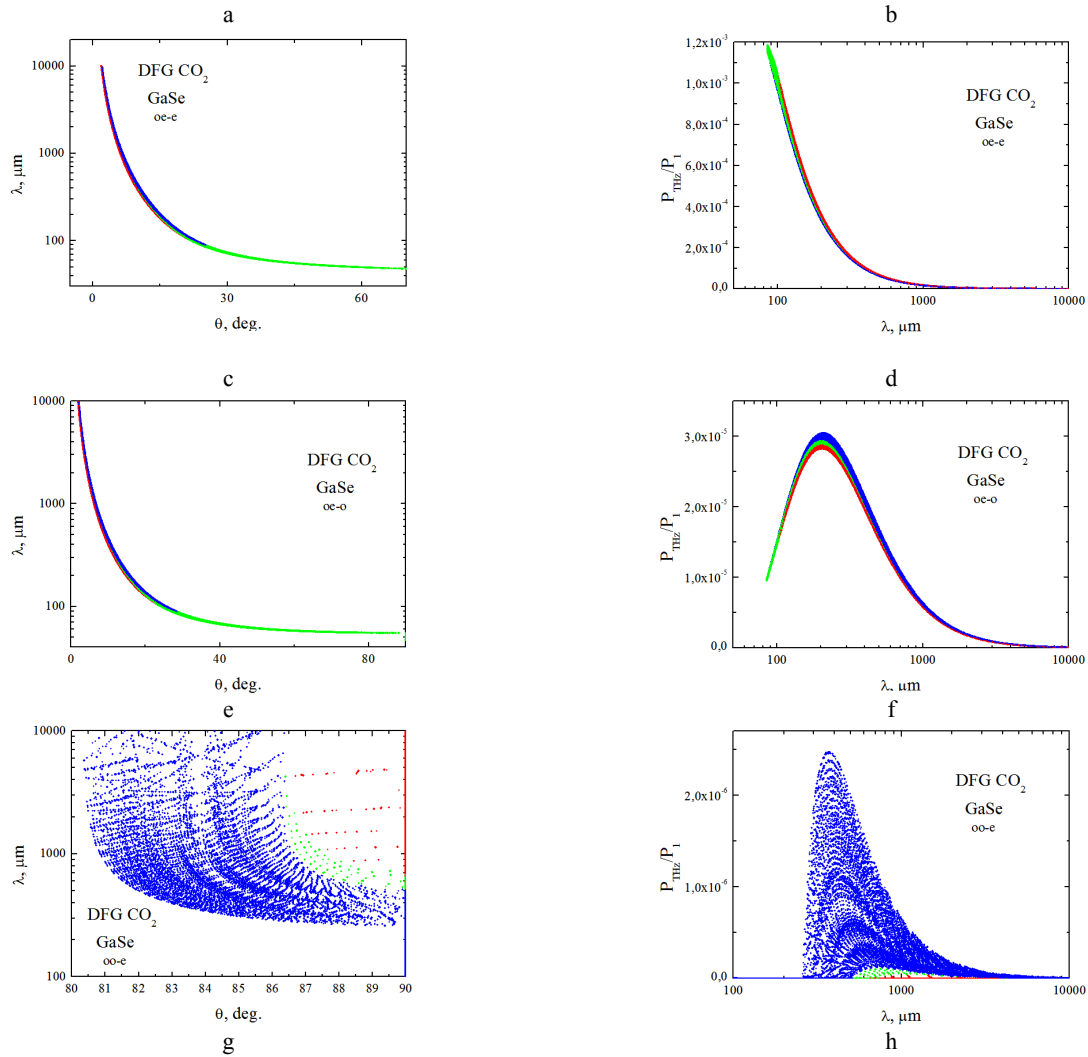


Fig. 2. Curves of DFG (a, c, e, g) PM and (b, d, f, h) frequency conversion efficiency  $P_{THz}/P_1$  in GaSe crystal under the pumping by two-frequency  $CO_2$  laser lines operating at:  $9 \mu m$  (red points),  $10 \mu m$  (blue points) and  $9 \mu m$  (first line) and  $10 \mu m$  (second line). Interaction types are identified in the figure insets.

In Fig. 2 it is seen that original ee-e type of DFG PM can be realized but with very low efficiency due to dominant absorption for e-wave over that for o-wave and also due to large (about  $90^\circ$ ) phase matching angle that minimizing  $d_{eff}$ . It can be proposed that this type of PM is preferable for short-wavelength pumping because much smaller PM angles. Besides, in Fig. 2 it is seen that oe-e type of interaction is the most efficient interaction for GaSe due to minimal phase mating angles and minimal absorption for e-wave in THz range. We found that original oo-o type of interaction is not possible to realize.

For clearness, two types of 3-d FDG PM curves and scaled figure of merit  $M = \frac{d_{eff}^2}{n_{p1} \cdot n_{p2} \cdot n_{THz}}$  are shown in Fig. 3;  $n_{p1, p2, THz}$  are refractive indices for interacting waves.

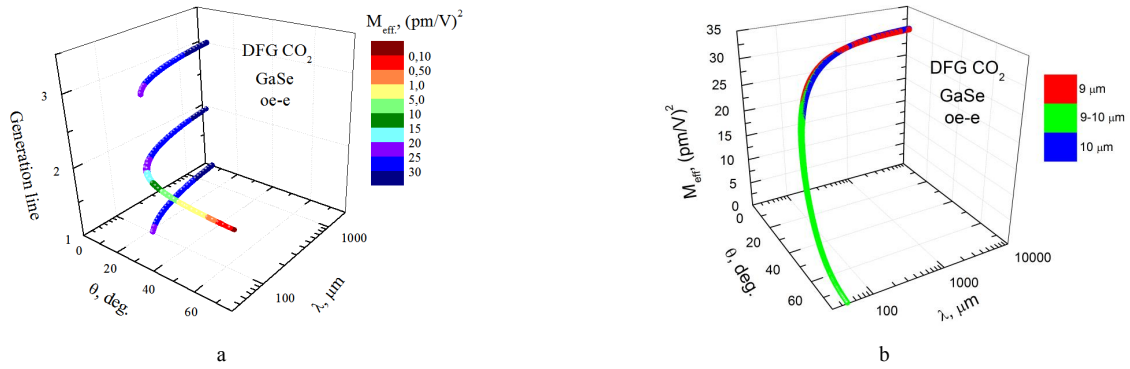
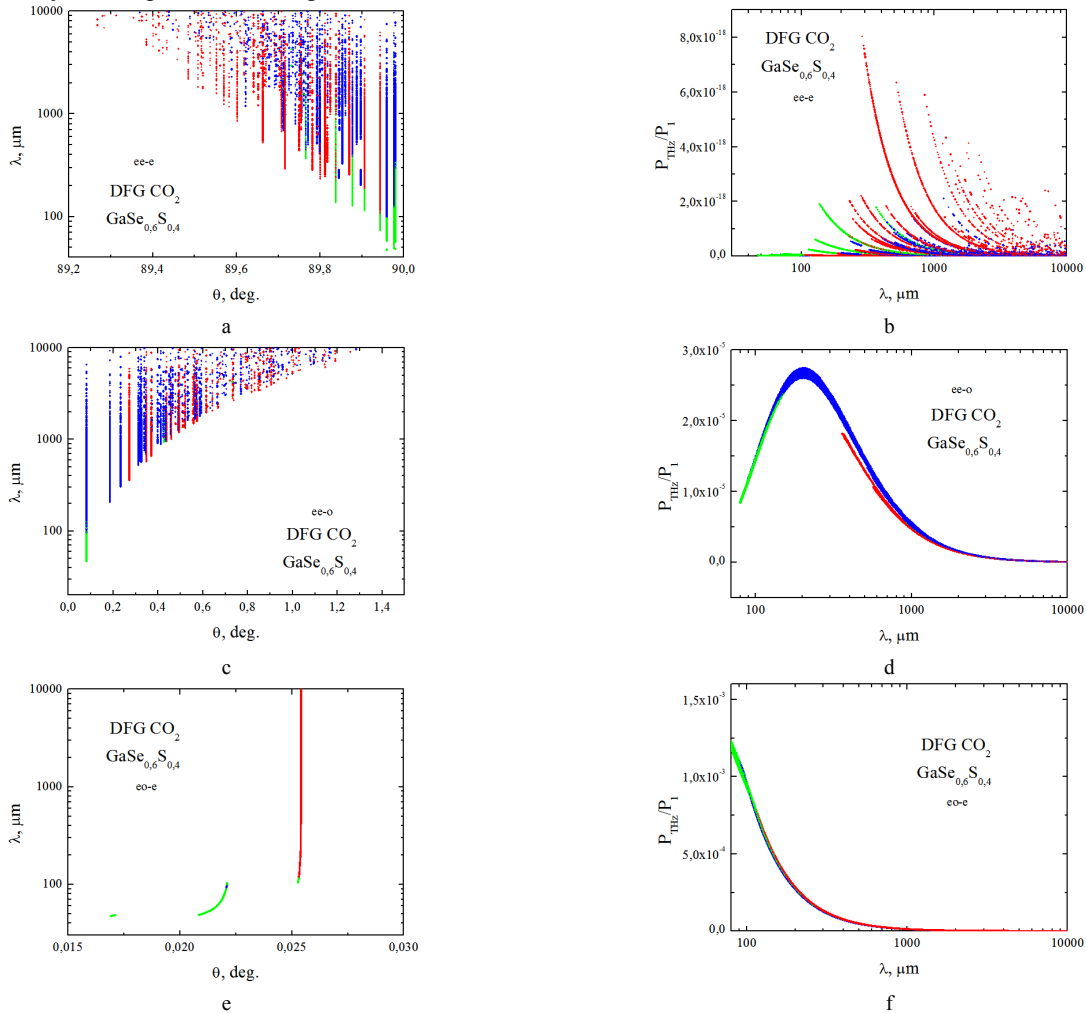


Fig. 3. Three-dimension (a) PM and (b) figure of merit  $M$  for  $\text{CO}_2$  laser line DFG in GaSe. Color  $M$ -scale and band of mixed emission lines are identified in the figure insets.

Figure of merit is proportional to frequency conversion efficiency. Fig. 3 allows rapid analyses of  $\text{CO}_2$  laser lines DFG into THz range by visual inspection.

For the first time such calculations are carried out for solid solution  $\text{GaSe}_{1-x}\text{S}_x$  crystals. In these calculations a decrease in  $d_{22}$  magnitude with S-doping as weighted average value for GaSe and GaS is accounted. Some calculation results for  $\text{GaSe}_{0.6}\text{S}_{0.4}$  crystal are presented in Fig. 4.



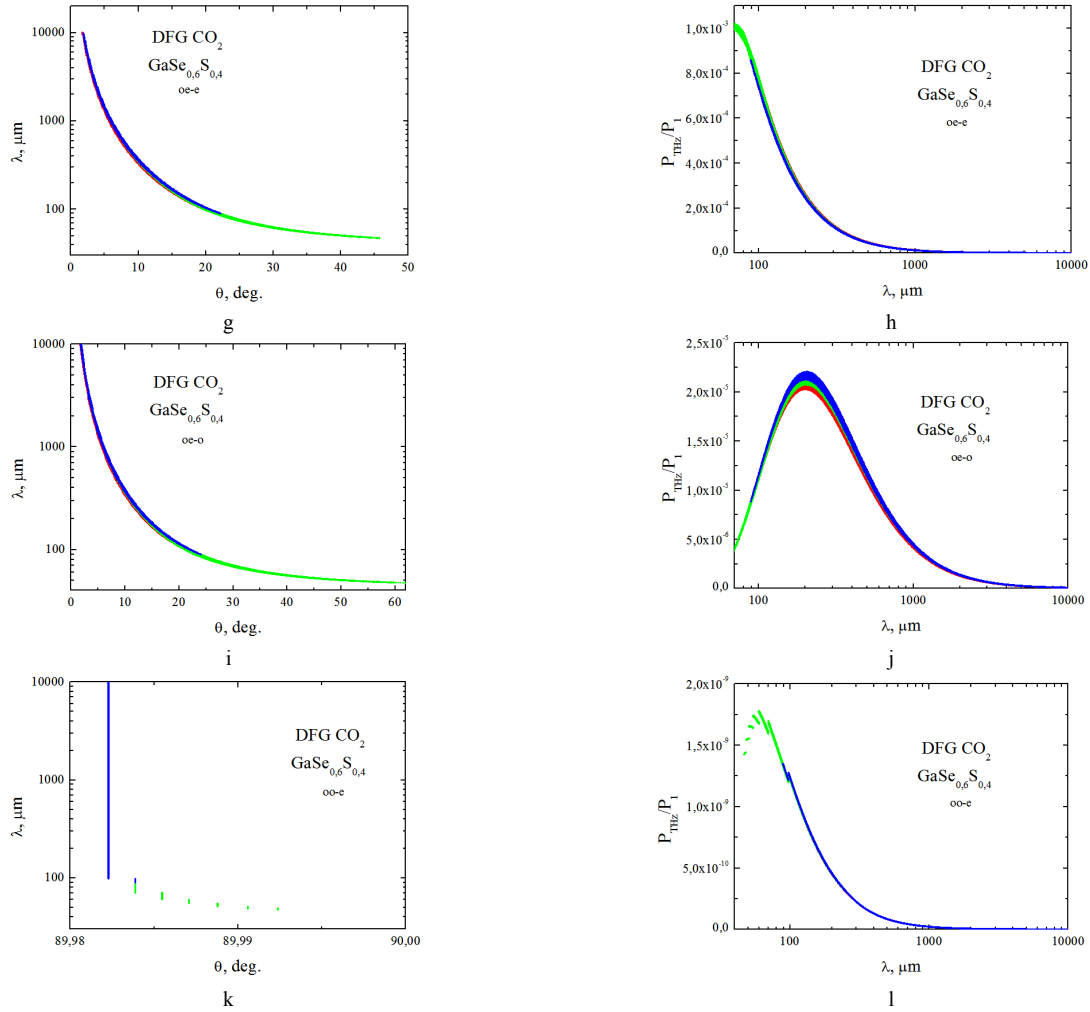


Fig. 4. Curves of DFG (a, c, e, g, i, k) PM and (b, d, f, h, j, l) frequency conversion efficiency  $P_{THz}/P_1$  in  $\text{GaSe}_{0.6}\text{S}_{0.4}$  crystal under the pumping by two-frequency  $\text{CO}_2$  laser lines operating at:  $9 \mu\text{m}$  (red points),  $10 \mu\text{m}$  (blue points) and  $9 \mu\text{m}$  (first line) and  $10 \mu\text{m}$  (second line). Interaction types are identified in the figure insets.

Three-dimensional PM curves and scaled figure of merits were calculated for solid solution crystals (Fig. 5) similar to that for GaSe.

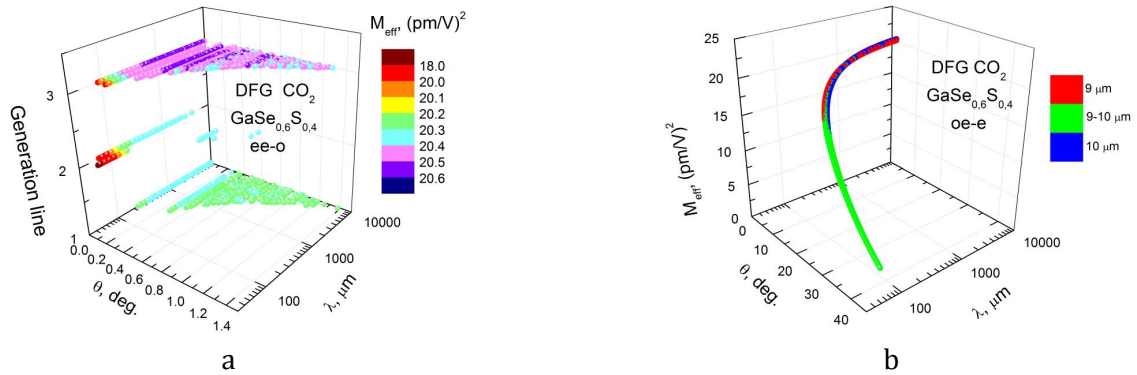


Fig. 5. Three-dimensional (a) PM and (b) figure of merit  $M$  for  $\text{CO}_2$  laser line DFG in  $\text{GaSe}_{0.6}\text{S}_{0.4}$ . Color  $M$ -scale and band of mixed emission lines are identified in the figure insets.

From the comparison it can be concluded that optimally doped ( $x = 0.09-0.13$ ) solid solution crystals  $\text{GaSe}_{1-x}\text{S}_x$  are from 4 to 5 times higher efficiency in THz generation in spite of lower nonlinearity if account higher damage threshold<sup>32</sup>. Backward DFG covers longer wavelength range to that by forward DFG that is attractive for practice due to absence of water vapor absorption lines.

## CONCLUSION

For the first time detailed model study of THz generation in pure and solid solution  $\text{GaSe}_{1-x}\text{S}_x$  crystals by  $\text{CO}_2$  laser down-conversion is carried out. Mixing of 9- $\mu\text{m}$  and 10- $\mu\text{m}$  band lines, as well cross band mixing is considered. Both forward and backward collinear interactions of common (eo-e, oe-e, oe-o, oo-e, ee-o) and original (ee-e, oo-o) types are analyzed. Dispersion properties of o- and e-wave refractive indices and absorption coefficients for GaSe, GaS and  $\text{GaSe}_{1-x}\text{S}_x$  crystals were preliminary measured by THz-TDS, approximated in the equation form and then used in the study. Improved quality crystals were grown by modified technology and used in these measurements. It was found that THz generation is possible up to mixing ratio  $x=0.5$ ; ee-e type of PM can be realized in difference to that for oo-o type but possesses low efficiency due to large PM angles that minimizes efficient nonlinearity and dominant absorption for pump e-wavelengths. eo-e type of interaction is the most efficient due to small PM angles and minimal absorption for THz e-waves. Estimated results are presented in the form of 3-D figures that are suitable for rapid analyses of DFG parameters.

**Acknowledgment:** The authors are grateful for partial financial support to RFBR Project No.12-02-33174.

## REFERENCES

- [1] Tekavec P., "Fixed 0.85/1.5 and tunable 0.8-2.8 THz source ideal for spectroscopy," *Laser Focus World*, 47 (11), 12 (2011).
- [2] Boyd G.D., Bridges T.J., Patel C.K.N., Buehler E., "Phase-matched submillimeter wave generation by difference-frequency mixing in  $\text{ZnGeP}_2$ ," *Appl. Phys. Lett.* 21 (11), 553-555 (1972).
- [3] Andreev Yu.M., Apollonov V.V., Shakir Yu.A., Verozubova G.A., Gribenyukov A.I., "Submillimeter-wave generation with  $\text{ZnGeP}_2$  crystals," *J. Korean Phys. Soc.* 33 (3), 320-325 (1998).
- [4] Ding Y. J., Shi W., "Widely tunable monochromatic THz sources based on phase-matched difference-frequency generation in nonlinear-optical crystals: A novel approach," *Las. Phys.* 16 (4), 562-570 (2006).
- [5] Yun-Shik Lee, [Principle of terahertz science and technology], Springer, New York, 340 (2008).
- [6] Apollonov V.V., Lebedev S.P., Komandin G.A., Shakir Yu.A., Badikov V.V., Andreev Yu.M., Gribenyukov A.I., "High power  $\text{CO}_2$ -laser radiation conversion with  $\text{AgGaSe}_2$  and  $\text{AgGa}_{1-x}\text{In}_x\text{Se}_2$  crystals," *Las. Phys.* 9 (6), 1236-1239 (1999).
- [7] Singh N.B., Norris T.B., Buma T., Singh R.N., Gottlieb M., Suhre D., Hawkins J.J., "Properties of nonlinear optical crystals in the terahertz wavelength region," *Opt. Engin.* 45 (9), 094002 (2006).
- [8] Kador L., Haarer D., Allakhverdiev K.R., Salaev E.Yu., "Phase-matched second-harmonic generation at 789.5 nm in a GaSe crystal," *Appl. Phys. Lett.* 69 (6), 731-733 (1996).
- [9] Wei Shi and Yujie J. Ding "A monochromatic and high-power terahertz source tunable in the ranges of 2.7–38.4 and 58.2–3540  $\mu\text{m}$  for variety of potential applications," *Appl. Phys. Lett.* 84 (10), 1635-1637 (2004).
- [10] Qu Y., Kang Z.-H., Wang T.-J., Jiang Y., Andreev Y.M., Gao J.-Y., "The detection of carbon monoxide by the second harmonic generation of  $\text{CO}_2$  laser," *Laser Phys. Lett.* 4 (3), 238-241 (2007).
- [11] Allahverdiev K.R., Guliev R.I., Salaev E.Yu., Smirnov V.V., "Investigation of linear and nonlinear optical properties of  $\text{GaS}_x\text{Se}_{1-x}$  crystals," *Quantum Electronics* 12 (7), 947-948 (1982).
- [12] Zhang H.-Z., Kang Z.-H., Jiang Yu., Gao J.-Yu., Wu F.-G., Feng Z.-S., Andreev Yu.M., Lanskii G.V., Morozov A.N., Sachkova E.I., Sarkisov S.Yu., "SHG phase matching in GaSe and mixed  $\text{GaSe}_{1-x}\text{S}_x$ ,  $x \leq 0.412$ , crystals at room temperature," *Opt. Exp.* 16 (13), 9951-9957 (2008).
- [13] Luo Z.-W., Gu X.-A., Zhu W.-C., Tang W.-C., Andreev Yu., Lanskii G., Morozov A., Zuev V., "Optical properties of GaSe:S crystals in terahertz frequency range," *Opt. Precision Eng.* 19 (2), 354-359 (2011).
- [14] Zhang L.-M., Guo J., Li D.-J., Xie J.-J., Andreev Yu.M., Gorobets V.A., Zuev V.V., Kokh K.A., Lanskii G.V., Petukhov V.O., Svetlichnyi V.A., Shaiduko A.V., "Dispersion properties of  $\text{GaSe}_{1-x}\text{S}_x$  in the terahertz range," *J. Appl. Spectr.* 77 (6), 850-856 (2011).
- [15] Sarkisov S.Yu., Nazarov M.M., Shkurinov A.P., Tolbanov O.P., " $\text{GaSe}_{1-x}\text{S}_x$  and  $\text{GaSe}_{1-x}\text{Te}_x$  solid solutions for terahertz generation and detection," *Proc. of the 34th Int. Conf. on Infrared, Millimeter and Terahertz wave*



(IRMMW-THz-2009). 21-25 September, 2009. Busan, Korea, (2009).

- [16] Suhre D. R., Singh N. B., Balakrishna V., Fernelius N. C., Hopkins F. K., "Improved crystal quality and harmonic generation in GaSe doped with indium," *Opt. Lett.* 22 (11), 775-777 (1997).
- [17] Singh N.B., Suhre D.R., Rosch W., Meyer R., Marable M., Fernelius N.C., Hopkins F.K., Zelmon D.E., Narayanan R., "Modified GaSe crystals for mid-IR applications," *J. Cryst. Growth* 198, 588-592 (1999).
- [18] Mandal K.C., Kang S.H., Choi M., Chen J., Zhang X.-C., Schleicher J.M., Schmuttenmaer C.A., Fernelius N.C., "III-VI chalcogenide semiconductor crystals for broadband tunable THz sources and sensors," *IEEE J. Select. Topics Quant. Electron.* 14 (2), 284-288 (2008).
- [19] Feng Z.-S., Kang Z.-H., Wu F.-G., Gao J.-Yu., Jiang Yu., Zhang H.-Z., Andreev Yu.M., Lanskii G.V., Atuchin V.V., Gavrilova T.A., "SHG in doped GaSe:In crystals," *Opt. Exp.* 16 (13), 9978-9985 (2008).
- [20] Rak Zs., Mahanti S.D., Mandal K.C., Fernelius N.C., "Doping dependence of electronic and mechanical properties of GaSe<sub>1-x</sub>Te<sub>x</sub> and Ga<sub>1-x</sub>In<sub>x</sub>Se from first principles," *Phys. Rev. B* 82, 155203 (2010).
- [21] Andreev Yu.M., Lanskii G.V., Orlov S.N., Polivanov Yu.N., "Physical properties, phase matching and frequency conversion in GaSe<sub>1-x</sub>S<sub>x</sub>, Ga<sub>1-x</sub>In<sub>x</sub>Se and GaSe<sub>1-x</sub>Te<sub>x</sub>," XVII Int. Conf. On Advanced Laser Technol., 26 Sep. - 1 Oct. 2009, Kosaeli, Turkey, 55 (2009).
- [22] Evtodiev I., Leontie L., Caraman M., Stamate M., Arama E., "Optical properties of p-GaSe single crystals doped with Te," *J. Appl. Phys.* 105, 023524 (2009).
- [23] Chen Ch.-W., Hsu Yu-K., Huang J.Y., Chang Ch.-Sh., Zhang Ji.-Yu., Pan Ci-L., "Generation properties of coherent infrared radiation in the optical absorption region of GaSe crystal" *Opt. Exp.* 14 (22), 10636-10644 (2006).
- [24] Yu-Kuei Hsu, Ching-Wei Chen, Jung Y. Huang, Ci-Ling Pan, Jing-Yuan Zhang, Chen-Shiung Chang, "Erbium doped GaSe crystal for mid-IR applications," 14 (12), 5484-5491 (2006).
- [25] Zhang Y.-F., Wang R., Kang Z.-H., Qu L.-L., Jiang Y., Gao J.-Y., Andreev Yu.M., Lanskii G.V., Kokh K.A., Morozov A.N., Shaiduko A.V., Zuev V.V., "AgGaS<sub>2</sub>- and Al-doped GaSe crystals for IR applications," *Opt. Commun.* 284, 1677-1681 (2011).
- [26] Ku S.-A., Chu W.-C., Luo C.-W., Andreev Y.M., Lanskii G., Shaiduko A., Izaak T., Svetlichnyi V., Wu K.H., Kobayashi T., "Optimal Te-doping in GaSe for non-linear applications," *Opt. Exp.* 20 (5), 5029-5037 (2012).
- [27] Xie Ji-Jiang, Guo Jin, Zhang Lai-Ming, Chen Fei, Jiang Ke, Andreev Yu.M., Atuchin V.V., Gorobets V.A., Lanskii G.V., Svetlichnyi V.A., Shaiduko A.V., "Frequency conversion of nanosecond CO<sub>2</sub>-laser into THz range in doped GaSe crystals," *Basic Problems Mat. Sci.* 9 (4), 486-494 (2012).
- [28] Jingguo Huang, Zhiming Huang, Jingchao Tong, Cheng Ouyang, Junhao Chu, Yury Andreev, Konstantin Kokh, Grigory Lanskii, Anna Shaiduko, "Intensive terahertz emission from GaSe<sub>0.91</sub>S<sub>0.09</sub> under collinear difference frequency generation," *Appl. Phys. Lett.* 103, 81104 (2013).
- [29] Sitnikov A.G., Panchenko A.N., Tel'minov A.E., Genin D.E., Sarkisov S.Yu., Bereznaya S.A., Korotchenko Z.V., Kazakov A.V., "Single-pulse CO<sub>2</sub> laser with frequency doubler based on GaSe and GaSe<sub>0.7</sub>S<sub>0.3</sub> single crystals," *Int. Symp. on High Current Electronics*, 586-588 (2010).
- [30] Rud V.Yu., Rud Yu.V., Vaipolin A.A., Bodnar I.V., Fernelius N., "Photosensitive structures on CdGa<sub>2</sub>S<sub>4</sub> single crystals," *Semiconductors* 37(11), 1321-1328 (2003).
- [31] Kokh K.A., Andreev Yu.M., Svetlichnyi V.A., Lanskii G.V., Kokh A.E., "Growth of GaSe and GaS single crystals," *Cryst. Res. Technol.* 46 (4), 327-330 (2011).
- [32] Feng Z.-S., Kang Z.-H., Li X.-M., Gao J.-Y., Andreev Yu. M., Atuchin V.V., Kokh K. A., Lanskii G. V., Potekaev A.I., Shaiduko A.V., Svetlichnyi V.A., "Impact of fs and ns pulses on solid solution crystals Ga<sub>1-x</sub>In<sub>x</sub>Se and GaSe<sub>1-x</sub>S<sub>x</sub>," *AIP Advances* 4(3), 037104 (2014).
- [33] Molloy J.F., Naftaly M., Andreev Yu.M., Lanskii G.V., Lapin I.N., Potekaev A.I., Kokh K.A., Shabalina A.V., Shaiduko A.V., Svetlichnyi V.A., "Dispersion properties of GaS studied by THz-TDS," *CrystEngComm.* 16 (10), 1995-2000 (2014).
- [34] Chen C.-W., Tang T.-T., Lin S.-H., Huang J.Y., Chang C.-S., Chung P.-K., Yen S.-T., Pan C.-L., "Optical properties and potential applications of ε-GaSe at terahertz frequencies," *J. Opt. Soc. Am. B* 26 (9), A58-A65 (2009).
- [35] Takaoka E., Kato K., "90° phase-matched third-harmonic generation of CO<sub>2</sub> laser frequencies in AgGa<sub>1-x</sub>In<sub>x</sub>Se<sub>2</sub>," *Opt. Lett.* 24 (13), 902-904 (1999).
- [36] Yariv A., [Quantum Electronics], Wiley, New York, 401 (1988).
- [37] Guo J., Li D-J, Xie J-J, Zhang L-M, Feng Z-S, Andreev Yu M, Kokh K A, Lanskii G V, Potekaev A I, Shaiduko A V and Svetlichnyi V A, "Limit pump intensity for sulfur-doped gallium selenide crystals," *Laser Phys. Lett.* 11 (5), 055401 (2014).